Desalination and Water Treatment
www.deswater.com

doi:10.5004/dwt.2017.0070

61 (2017) 12–19
January

Fouling behaviors of membrane distillation (MD) in shale gas wastewater treatment

Hyeongrak Cho[a], Yonghyun Shin[a], Yongjun Choi[a], Sangho Lee[a,*], Jinsik Sohn[a], Dongha Kim[a], Jaewuk Koo[a,b]

[a]*School of Civil and Environmental Engineering, Kookmin University, 77 Jeongneung-ro, Seongbuk-gu, Seoul, 02707, Korea, Tel. +82-2-910-4529, Fax +82-2-910-4939, email: sanghlee@kookmin.ac.kr*
[b]*Korea Institute of Civil Engineering and Building Technology, 283, Goyang-daero, Ilsanseo-gu, Goyang-si, Gyeonggi-do, 10223, Korea*

Received 19 January 2016; Accepted 24 August 2016

ABSTRACT

One of the major environmental risks of shale gas development is water contamination caused by hydraulic fracturing, resulting in the generation of high salinity wastewaters. During the shale gas wastewater treatment, there are typically multi-step treatment processes, including candidates such as air flotation, biological treatment, and chemical coagulants. In this paper, membrane distillation (MD) technique with simple and economical pre-treatment was applied to treat the shale gas wastewaters containing more than 300,000 mg/L total dissolved solids with porous hollow fiber membranes. In addition, fouling mechanisms in the MD treatment of the wastewaters were explored using a theoretical model based on the crystallization theory. From the laboratory results, it was found that the flux decline due to scale formation was the serious problem in the treatment of the real wastewaters. The analysis of the MD membrane surfaces using scanning electron microscopy and X-ray photoelectron spectroscopy revealed the morphologies and compositions of the foulant layers after the MD treatment.

Keywords: Shale gas; Membrane distillation; Flat sheet membrane; Hollow fiber membrane; Produced water; Fouling mechanism

1. Introduction

As interest in shale gas has spread all over the world, there is a growing concern on its environmental impact [1–3]. The potential for natural water contamination is high when producing shale gas through hydraulic fracturing [3–5]. It has been recently reported that flow back and produced waters from Haynesville (Texas) and Marcellus (Pennsylvania) shale have high salinity (>200,000 mg/L total dissolved solids [TDS]) concentrations [4]. Moreover, proppant and toxic organic and inorganic chemicals are included in such wastewaters [4,6,7]. Accordingly, it is difficult to properly treat the shale gas wastewaters by conventional wastewater treatment techniques [7].

A few novel techniques have been proposed for the treatment of shale gas wastewater [8], including such as multi-effect distillation (MED), mechanical vapor compression (MVC), forward osmosis (FO) [9,10], and membrane distillation (MD) [5,6]. Of particular interest in this study is MD that have ability to treat feed waters with high salinity [11,12]. MD uses thermal energy for the separation of fresh water from saline water [13]. A hydrophobic microporous membrane is an essential part of this system because it provides a barrier to separate a hot feed water and a cold product water [5]. The advantages of MD over other wastewater treatment techniques includes [6,11,14–16]: low electricity requirement; ability to be operated under low temperature and pressure conditions; integration with renewable energy

*Corresponding author.

Presented at the 8th International Conference on Challenges in Environmental Science & Engineering (CESE-2015), 28 September–2 October 2015, Sydney, Australia.

sources such as waste heat and solar thermal energy; small footprint; and capability to remove non-volatile impurities including ions, polymers, and colloids.

However, one of the major challenges in MD is flux decline and permeability loss due to membrane fouling [15]. Considering that there are substantial amount of salts in the shale gas wastewater, scale formation may occur on the surface of MD membranes, resulting in a reduction in the performance of the process and an increase in operation costs [17]. In addition to scale formation, organic matters and colloidal particles may also cause fouling in MD. Accordingly, it is imperative to control MD fouling for its application to the treatment of shale gas wastewater.

Scale formation is not only a problem in MD but also a problem in other membrane systems such as reverse osmosis (RO) and nanofiltration (NF). Accordingly, a handful of researches have been presented in the literature for the control of the scale formation in membrane systems. Soluble inorganic salts including calcium carbonate, calcium sulfate, barium sulfate, and silica cause scale formation in membrane systems [18–20], resulting in permeability loss of membranes and damage of membrane structures [17,21]. Several methods have been established to control scale formation, including acid addition, softening, and the use of antiscalant [17,22,23]. Especially, antiscalants are found to be effective to control scale formation in NF/RO processes due to their ability to prolong the induction time for the crystallization [22,24,25]. Threshold inhibition is another representing aspect of antiscalants [15]. Membrane crystallization is also an approach to control scale formation by continuously precipitating crystals during MD treatment [26–28]. While antiscalants modify the kinetics of crystallization, membrane crystallization relies on crystallization equilibrium.

Nevertheless, little information is available on fouling phenomena and scale formation mechanisms in MD treatment of shale gas wastewater. Accordingly, this study explored the mechanisms of fouling in MD systems for the treatment of high salinity wastewater from shale gas development. A series of MD experiments were carried out using laboratory-scale MD systems. A simple theoretical model based on the crystallization kinetics and surface blockage model was derived and applied to interpret the experimental results. The difference in fouling propensity between flat sheet and hollow fiber membranes was also investigated.

2. Model development

In this study, simple model equations were derived to examine the fouling due to scale formation in MD systems. In general, the rate of crystallization on the membrane surface is given by [29,30]:

$$\frac{dm_s}{dt} = kA_m\left(c - c^*\right)^n \tag{1}$$

where m_s is the mass of crystals formed on the membrane surface; t is the time; k is the rate constant for the crystallization, A_m is the membrane area, c is the bulk concentration, c^* is the saturation concentration, and n is the reaction order. In Eq. (1), m_s can be expressed as:

$$m_s = \rho V_s = \rho A_s \delta \tag{2}$$

where ρ is the density of crystals; V_s is the volume of surface crystals; A_s is the area of the surface crystals; and d is the thickness of the surface crystals. The formation of the surface crystals reduces the effective surface area of the membrane, thereby reducing the permeability of the membrane. Accordingly, the relative permeability β is:

$$\frac{A_m - A_s}{A_m} = \beta \tag{3}$$

Using Eqs. (1) and (3), the Eq. (4) can be derived:

$$\frac{d\beta}{dt} = -\frac{1}{A_m}\frac{dA_s}{dt} = -\frac{1}{\rho\delta A_m}\frac{dm_s}{dt} = -\frac{k}{\rho\delta}\left(c - c^*\right)^n \tag{4}$$

Rearranging Eq. (4), the following equation can be obtained:

$$\frac{d\beta}{dt} = -\frac{k}{\rho\delta}{c_0}^n\left(\frac{c}{c_0} - \frac{c^*}{c_0}\right)^n = -\alpha\left(\frac{c}{c_0} - \frac{c^*}{c_0}\right)^n \tag{5}$$

where c_0 is the initial bulk concentration. When no fouling occurs, the flux in MD can be generally given by [11]:

$$J_0 = B\Delta p \tag{6}$$

where J_0 is the pure water vapor flux; B is the apparent permeability of MD membrane; and Dp is the vapor pressure difference. If scale formation occurs, the flux decreases due to the reduction in effective surface area. Accordingly, the flux J is given by [31]:

$$J = \frac{A_m - A_s}{A_m}B\Delta p = \beta B\Delta p \tag{7}$$

In most crystallization processes, crystals are not immediately created even if supersaturation is achieved [29,30]. Instead, an interval is required before the onset of the crystallization, which is called as induction time [31]. This implies that MD flux decline may not occur from the beginning even if the feed solution is supersaturated. Accordingly, the final model equation for flux decline due to scale formation in MD is:

$$\begin{aligned} J &= B\Delta p && 0 < t < t_{ind} \\ J &= \beta B\Delta p = J_0\int_{t_{ind}}^{t} -\alpha\left(\frac{c}{c_0} - \frac{c^*}{c_0}\right)^n dt && t > t_{ind} \end{aligned} \tag{8}$$

3. Materials and methods

3.1. Feed waters

Two feed waters were used to investigate the fouling mechanisms in MD during the treatment of shale gas wastewater. Produced water from a shale gas well in Bakken, Williston, was obtained and applied. Prior to the MD experiments, the wastewater was pre-treated using a sediment filter and a pre-carbon filter. Together with the real wastewater, a synthetic wastewater was also prepared and used. The composition of the synthetic wastewater was determined based on that of the real wastewater.

Table 1
Compositions of real wastewater

Parameter	Value
pH	5.5
Total alkalinity (ppm as $CaCO_3$)	76
Total suspended solids (ppm)	3134
Total dissolved solids (ppm)	357,500
Volatile suspended solids (ppm)	343
Total solids (ppm)	360,600
Turbidity (NTU)	454
Conductivity (μS cm^{-1})	259,000
Total phosphorus (ppm)	79
Oil and grease, HEM (ppm)	84
Oil and grease, SGT-HEM (ppm)	46
Total hardness (ppm as $CaCO_3$)	64,300
Hardness, calcium (ppm as $CaCO_3$)	31,400
Dissolved oxygen (ppm)	7
Chemical oxygen demand (ppm)	15,820
Total organic carbon (ppm)	1420
Sulfide (ppm)	0.3

Table 2
Composition of synthetic wastewater

Salts	Concentration (mg/L)
NaCl	240,000
$CaCl_2$	51,300
KCl	13,300
$MgCl_2$	3,200
TDS	307,800
Conductivity	241,000 (μS cm^{-1})

Major ions in the real wastewater including Na^+ (27.2% of the TDS), Cl^- (52.3%), K^+ (1.94%), Mg^{2+} (0.36%), and Ca^{2+} (5.18%) were selected for the synthetic wastewater. The water quality parameters for these wastewaters are listed in Tables 1 and 2.

These wastewaters were pre-treated prior to MD experiments. The real wastewater and the synthetic wastewater were treated using a multi-media filter and a GF/C filter, respectively. After the pre-treatment, the turbidity of the real wastewater was reduced to 4.5 NTU. Nevertheless, the TDS and conductivity were not significantly changed. The turbidity of the real wastewater decreased to less than 1 NTU after the treatment.

3.2. Membranes

Hollow fiber (Econity, Korea) membranes were compared in this study. According to the membrane manufacturer, the pore diameter of the membranes ranged from 0.2 to 1.0 mm, and the porosity was 75%. The inner diameter and outer diameter of the fibers were 0.7 and 1.3 mm, respectively. The membrane area for the hollow fiber membranes was 0.0125 m^2.

3.3. Experimental setup

Two laboratory-scale systems for direct contact membrane distillation (DCMD) and vacuum membrane distillation (VMD) were used to measure water vapor flux. Details on the experimental systems were reported in our previous study [32]. As shown in Fig. 1, each has a membrane module, a feed tank, a distillate (permeate) tank, a heater, an electronic balance, and a gear pump for the recirculation of the feed solution. In the DCMD system (Fig. 1a), a cooler was attached to the distillate side to maintain constant temperature (20°C). In the VMD system (Fig. 1b), a condenser was used to convert water vapor to liquid water. In both systems, temperatures in feed and permeate sides were controlled using a water bath. Moreover, the recirculation flow rates ranged from 0.2 to 1.6 L min^{-1}. A hollow fiber membrane module was used for each experiment. The conditions for the MD experiments are summarized in Table 3.

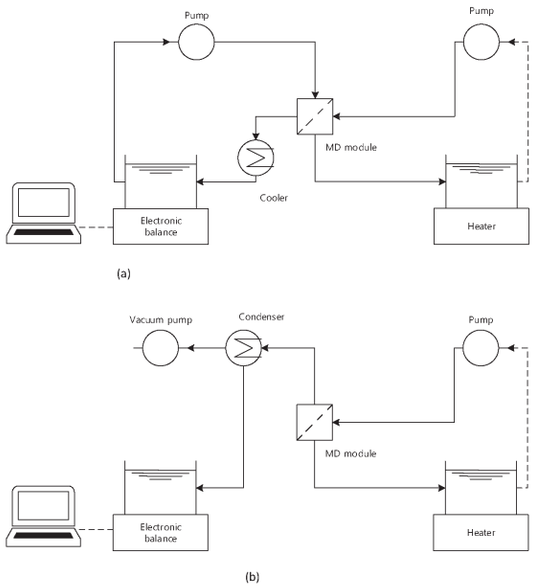

Fig. 1. Schematic diagram for laboratory-scale DCMD and VMD systems.

Table 3
Summary of experimental conditions for hollow fiber membranes

Item		Condition
Operation type		DCMD, VMD
Membrane		PVDF 0.2–1.0 μm, 75% porosity
Effective membrane area		0.0125 m^2
Cross-flow velocity	Feed	0.6 L min^{-1}
	Permeate	0.4 L min^{-1}
Temperature	Feed side	60°C
	Permeate side (DCMD)	20°C
Vacuum	Permeate side (VMD)	100 mbar

3.4. Analysis of membrane surface

After the MD fouling experiments, the surfaces of the membranes were analyzed. A field-enhanced scanning electron microscope (FE-SEM, Hitachi S-4700, Korea) was used to examine the membrane surface of the scale phenomena on the membrane structure after the experiments. Membrane samples were completely dried at 50°C for 12 h in a dry oven and coated with platinum. In addition, X-ray photoelectron spectroscopy (XPS) was attempted to measure the elemental composition on the membrane surfaces after the MD fouling experiments.

4. Results and discussion

4.1. Synthetic wastewater

The MD experiments using the synthetic wastewater were conducted in order to investigate the effect of major ions such as Na^+, Ca^{2+}, K^+, Mg^{2+}, and Cl^- on membrane fouling due to scale formation. These results were compared with those using the real wastewater to investigate the effect of minor components. As shown in Fig. 2(a), only a slight decrease in flux was observed in the DCMD experiment. The initial flux was 6.0 kg m^{-2}-h^{-1}, and the final flux was 5.7 kg m^{-2}-h^{-1}, indicating the reduction in the permeability by 5%. The flux decline in the VMD experiment was also smaller: The initial flux was 9.83 kg m^{-2}-h^{-1}, and the final flux was 9.0 kg m^{-2}-h^{-1}. This suggests that the fouling due to scale formation is not significant in the conditions of synthetic wastewater experiments. This is attributed to the conditions of these experiments. In the beginning, the feed solution was almost saturated with salts. As the MD experiment proceeds, the solution becomes supersaturated, and the degree of the supersaturation is proportional to the volume concentration factor. However, the concentration factors for these experiments were less than 1.15, indicating that the rate of crystallization is not high based on Eq. (1). Moreover, the induction appears to be longer than the operation time under these conditions.

4.2. Real wastewater

Fig. 3 shows the changes in flux with time for the real wastewater. The results are quite different from those in Fig. 2. The flux decreased quite quickly as DCMD operation proceeded after 400 min as shown in Fig. 3(a). The initial flux was 7.9 kg m^{-2}-h^{-1}, and the final flux was

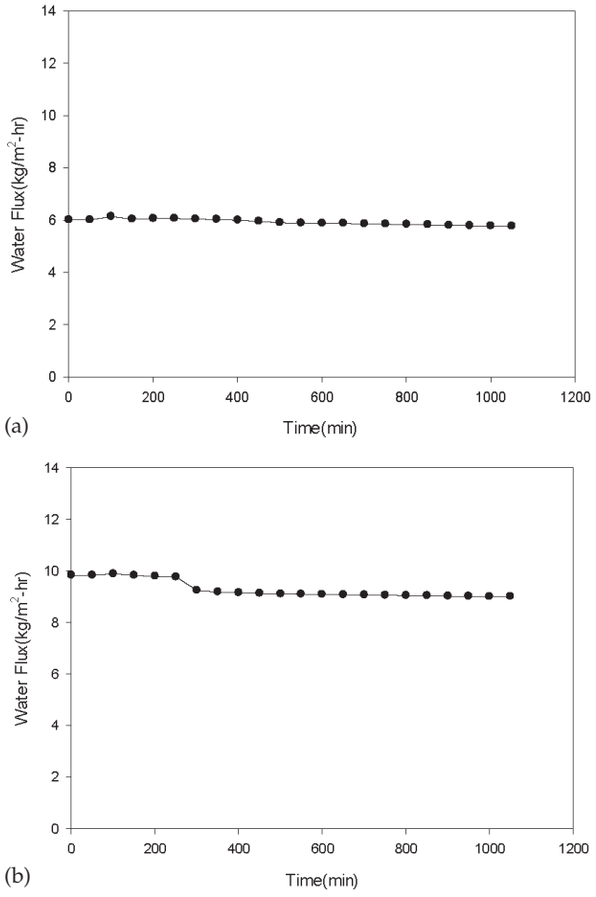

Fig. 2. Variations in water vapor flux with time for synthetic wastewater in DCMD and VMD systems: (a) DCMD and (b) VMD.

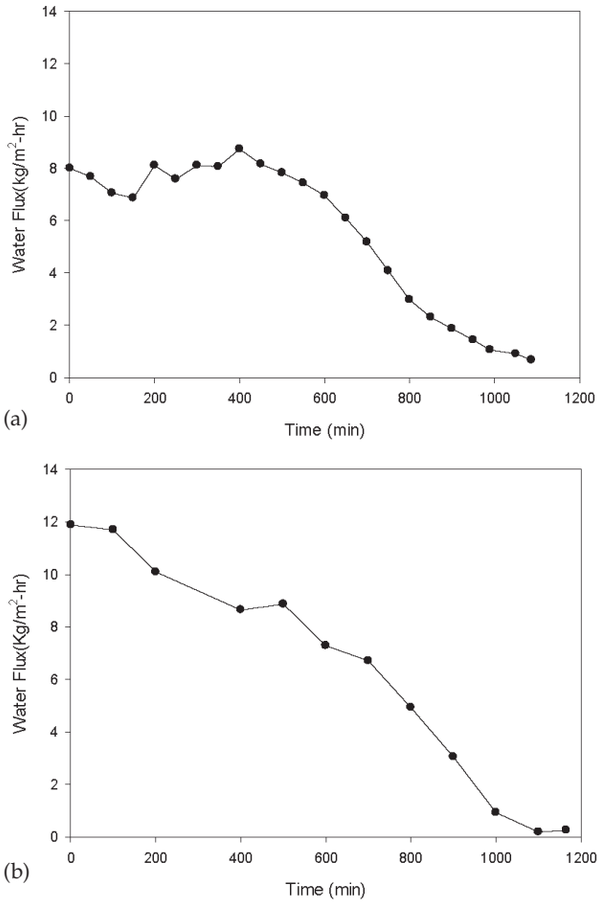

Fig. 3. Variations in water vapor flux with time for real wastewater in DCMD and VMD systems: (a) DCMD and (b) VMD.

0.67 kg m^{-2} h^{-1}, indicating the reduction in the permeability by 91.5%. The flux decline in VMD was more serious than that in DCMD as shown in Fig. 3(b). Although the initial flux was higher, the flux decreased from the beginning of the VMD operation. After 1000 min, the flux became lower than 1 kg m^{-2}-h^{-1}. It is evident that MD flux decline in the treatment of the real wastewater was substantial.

Although the TDS values for the synthetic and real wastewaters were similar, the initial flux values in Fig. 3 were smaller than those in Fig. 2. This is attributed to the inhomogeniety of the membranes from different batches. Since the membranes used for the synthetic wastewater and real wastewater were obtained from different batches, the initial flux values were different. The manufacturer of the membranes specifies a tolerance of ±10% for the initial flux in different batches, which explains the flux differences between the synthetic and real wastewaters (up to 2 kg m^{-2} h^{-1}). However, the membranes from the same batch was used for DCMD and VMD experiments with the same wastewater.

The different fouling potential between the synthetic wastewater and the real wastewater can be explained by their compositions and properties. The real wastewater contains not only salts but also other compounds such as dissolved organics and trace metal ions. Although their concentrations are relatively lower than those of salts such as NaCl, $CaCl_2$, and $MgCl_2$, they may affect the kinetics of nucleation and crystal growth, leading to accelerated formation of scales. In other words, the real wastewater seems to be less stable than the synthetic wastewater, which results in shorter induction time and higher rate of crystallization.

It should be pointed out from Fig. 3 that DCMD and VMD showed different flux behaviors. Since the initial flux in VMD is higher than that in DCMD, the rate of scale formation on the membrane surface is also higher due to high concentration of salts on the membrane surface. Similar results were also reported in NF membrane systems [33], which suggests that initial flux is also an important factor affecting the MD fouling due to scale formation.

4.3. Application of model equation

To further examine the scale formation in MD systems, the Eq. (8) was applied to the experimental results. The induction time t_{ind} was determined from the inflection point of the flux curves. The α values were determined from linear regression between $J_0\int_{t_{ind}}^{t}\left(c/c_0 - c^*/c_0\right)^n dt$ and J. Using the t_{ind} and a, the flux was estimated using the Eq. (8). The results using the synthetic wastewater are shown in Fig. 4. This figure compares the real flux with the calculated flux against time. Since this is a model fit, the best model fit parameter was determined from this plot. Moreover, the plot is linear, indicating that the model equation can used to quantify the fouling behaviors. Both the model calculations for DCMD and VMD showed good agreements with the experimental results. The R^2 values were 0.962 for DCMD and 0.970 for VMD, suggesting that the simple model can predict flux decline in MD for shale gas wastewater treatment.

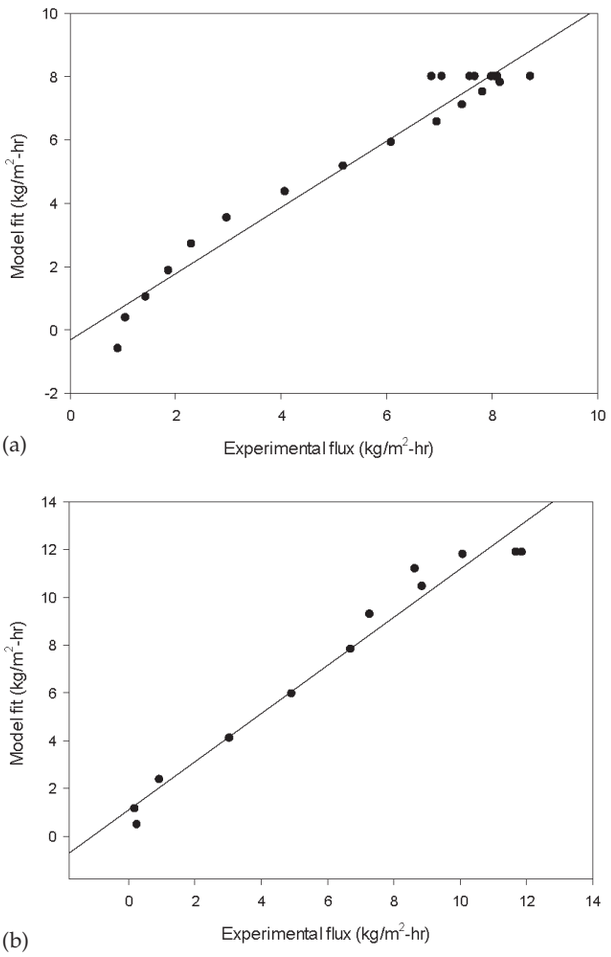

Fig 4. Comparison of model fits with experimental results using the real wastewater: (a) DCMD and (b) VMD.

Using the model, the fouling behaviors in MD can be described in terms of α and t_{ind}. From the model fits, the α for DCMD was found to be 0.303, which is lower than that for VMD (0.619). Since the α is related to the rate of fouling, a larger α in VMD indicates higher fouling propensity in VMD than that in DCMD.

Based on the flux profiles, the induction time for DCMD was found to be 400 min while that for VMD was 0 min. The induction time (or period) is defined as an initial slow stage of a crystallization reaction; after the induction time, the crystallization reaction accelerates. Accordingly, if the induction time is shorter, the crystallization reaction occurs faster. Accordingly, these results indicate that the fouling propensity is higher in VMD than in DCMD.

As pointed out, the higher flux in the initial stage of the operation in VMD is one of the reasons to cause this. There may be other factors affecting the fouling propensity, including the flow patterns, applied pressure, and existence of the vacuum on the distillate side. Further study will be required for in-depth analysis of the fouling mechanisms in DCMD and VMD systems.

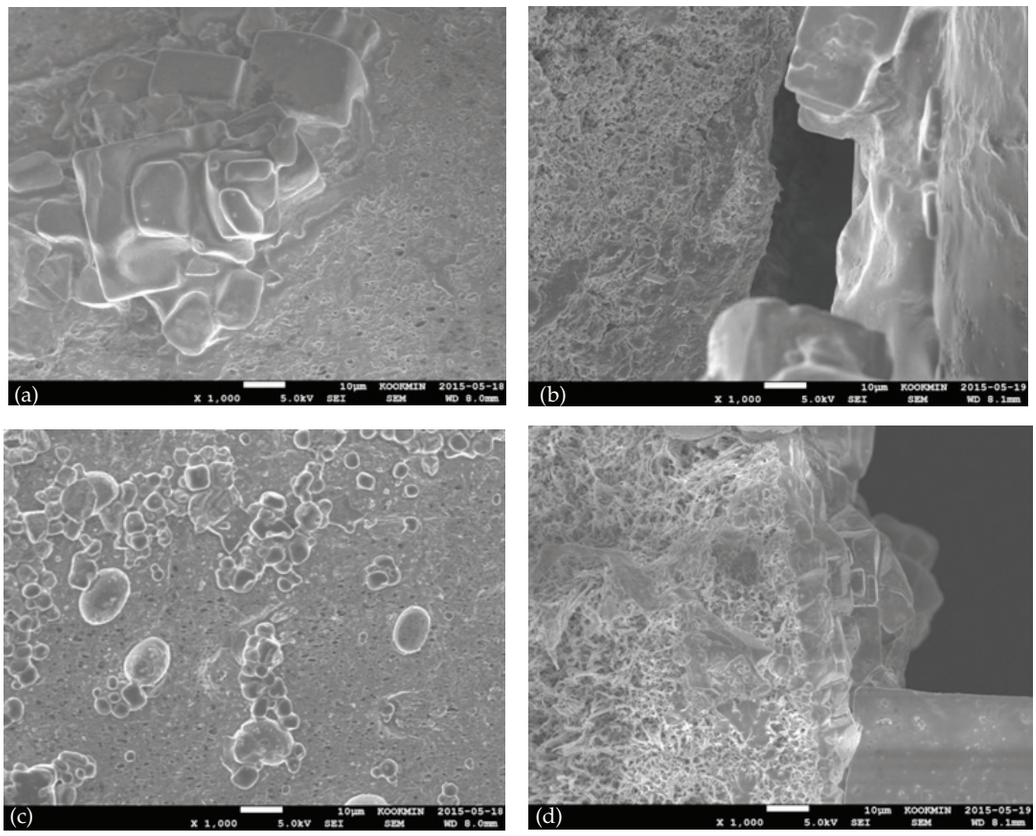

Fig. 5. SEM images after MD experiments: (a) DCMD, (b) DCMD membrane surface and cross section, (c) VMD, and (d) VMD membrane surface and cross section.

4.4. Analysis of fouling layers on membrane surface

The SEM analysis was applied to observe the scale formation on the membranes surfaces after the MD operation. Figs. 5(a) and 5(b) show the images of membrane surfaces after DCMD operation. It was found that the crystals were formed on the membrane surface and cross section. Moreover, it is likely that the crystals blocked the entrance of the pores. The flux after the MD operation was only 8.5% of the initial flux, implying that most pores are blocked by the crystals.

Figs. 5(c) and 5(d) show the images of membrane surface and cross section after VMD operation. Again, the crystal layers were found on the membrane surface. The morphology of the crystals formed in VMD seems to be different from that in DCMD. The size of crystals is generally smaller in VMD than in DCMD. The difference in crystal size between VMD and DCMD results from the different degree of concentration polarization caused by the initial flux. If the initial flux is higher, the salt concentration is higher due to higher permeation drag, resulting in higher salt concentration due to increased concentration polarization degree. Accordingly, the rate of crystallization is higher, and the crystal growth is enhanced.

The results of XPS analysis is shown in Fig. 6. There were six major peaks in the XPS plot: C1s (31.35%), Cl2p (33.73%), Na1s (13.43%), O1s (9.44%), Si2p (4.96%), and Ca2p (3.65%) in Table 4. The carbon peak seems to mainly originate from the membrane material. This can also be attributed to the organic carbons deposited on the membrane surface. Accordingly, it appears that the major foulants are NaCl, SiO_2, $CaCO_3$, and organic carbons. It should be noted that SiO_2, $CaCO_3$, and organic carbons were not included in the synthetic wastewater. This could be the reason why the fouling potential of the real wastewater was higher than that of the synthetic wastewater.

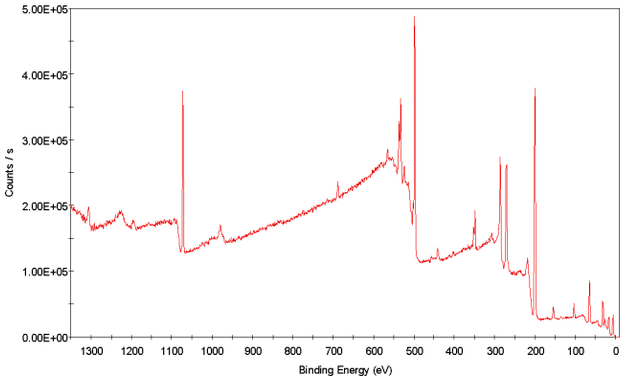

Fig. 6. XPS results after MD experiments.

Table 4
XPS peak mapping for membrane surface

Name	Peak BE	Area (P) CPS.eV	Area (N)	At. %	SF
C1s	284.88	34,790.76	493.81	31.35	1
Ca2p	348.22	19,894.91	57.54	3.65	5.07
Cl2p	199.44	89,150.14	531.42	33.73	2.285
F1s	687.79	7,247.08	29.67	1.88	4.43
N1s	399.4	1,448.7	12.13	0.77	1.8
Na1s	1,072.31	67,023.1	211.52	13.43	8.52
O1s	532.27	26,740.33	148.75	9.44	2.93
P2p	134.67	1,118.49	12.41	0.79	1.192
Si2p	102.37	4,895.03	78.13	4.96	0.817

5. Conclusions

In this study, fouling of hollow fiber MD membranes during the treatment of shale gas wastewater was investigated. The following conclusions were drawn:

- It was possible to stably operate the laboratory-scale MD with a minimal pre-treatment (sediment filter, pre-carbon filter, and MF) for removing total suspended solids and turbidity.
- When the synthetic wastewater was used, flux decline due to fouling was not significant. The results were similar in both DCMD and VMD except for the initial flux.
- However, the real wastewater showed higher fouling propensity than the synthetic wastewater. This is attributed to the difference in the compositions between the two wastewaters.
- A simple model considering the crystallization kinetics and surface blockage could predict the flux during the MD treatment. The model results revealed that the rate constant of the crystallization in DCMD was higher than that in VMD. The induction time was short in VMD, resulting in the immediate flux decline from the beginning.
- The morphological aspects of the crystals on the membrane surfaces were different between DCMD and VMD. Again, this is explained by the difference in the initial flux.
- The XPS results showed that the major foulants are NaCl, SiO_2, $CaCO_3$, and organic carbons. This could be the reason why the fouling potential of the real wastewater was higher than that of the synthetic wastewater.

Acknowledgment

This research was supported by a grant from Ministry of Trade, Industry and Energy of Korean government (Project Number: 10048900) and a grant (code 13IFIP-B065893-01) from Industrial Facilities & Infrastructure Research Program.

References

[1] USEIA, Annual Energy Outlook 2012 with Projections to 2035. Vol. DOE/EIA-0383 2012, Washington, DC: U.S. Energy Information Administration, U.S. Department of Energy.
[2] X. Zhang, A.Y. Sun, I.J. Duncan, Shale gas wastewater management under uncertainty, J. Environ. Manage., 165 (2016) 188–198.
[3] D. Zhang, T. Yang, Environmental impacts of hydraulic fracturing in shale gas development in the United States, Petrol. Explor. Develop., 42 (2015) 876–883.
[4] Y.K. Kharak, J.J. Thordsen, C.H. Conaway, R.B. Thomas, The energy-water nexus: potential groundwater-quality degradation associated with production of shale gas, Procedia Earth Planet. Sci., 7 (2013) 417–422.
[5] D. Singh, K.K. Sirkar, Desalination of brine and produced water by direct contact membrane distillation at high temperatures and pressures, J. Membr. Sci., 389 (2012) 380–388.
[6] H.W. Chung, J. Swaminathan, D.M. Warsinger, J.H. Lienhard V, Multistage vacuum membrane distillation (MSVMD) systems for high salinity applications, J. Membr. Sci., 497 (2016) 128–141.
[7] Q. Jiang, J. Rentschler, R. Perrone, K. Liu, Application of ceramic membrane and ion-exchange for the treatment of the flowback water from Marcellus shale gas production, J. Membr. Sci., 431 (2013) 55–61.
[8] G.P. Thiel, E.W. Tow, L.D. Banchik, H.W. Chung, J.H. Lienhard V, Energy consumption in desalinating produced water from shale oil and gas extraction, Desalination, 366 (2015) 94–112.
[9] B.D. Coday, P. Xu, E.G. Beaudry, J. Herron, K. Lampi, N.T. Hancock, T.Y. Cath, The sweet spot of forward osmosis: treatment of produced water, drilling wastewater, and other complex and difficult liquid streams, Desalination, 333 (2014) 23–35.
[10] J. Minier-Matar, A. Hussain, A. Janson, R. Wang, A.G. Fane, S. Adham, Application of forward osmosis for reducing volume of produced/process water from oil and gas operations, Desalination, 376 (2015) 1–8.
[11] A. Alkhudhiri, N. Darwish, N. Hilal, Membrane distillation: a comprehensive review, Desalination, 287 (2012) 2–18.
[12] J. Zuo, S. Bonyadi, T.S. Chung, Exploring the potential of commercial polyethylene membranes for desalination by membrane distillation, J. Membr. Sci., 497 (2016) 239–247.
[13] Y. Zhang, Y. Peng, S. Ji, Z. Li, P. Chen, Review of thermal efficiency and heat recycling in membrane distillation processes, Desalination, 367 (2015) 223–239.
[14] I. Hitsov, T. Maere, K. De Sitter, C. Dotremont, I. Nopens, Modelling approaches in membrane distillation: a critical review. Sep. Purif. Technol., 142 (2015) 48–64.
[15] L.D. Tijing, Y.C. Woo, J.-S. Choi, S. Lee, S.-H. Kim, H.K. Shon, Fouling and its control in membrane distillation—a review, J. Membr. Sci., 475 (2015) 215–244.
[16] M.A.E.-R. Abu-Zeid, Y. Zhang, H. Dong, L. Zhang, H.-L. Chen, L. Hou, A comprehensive review of vacuum membrane distillation technique, Desalination, 356 (2015) 1–14.
[17] H.C. Duong, S. Gray, M. Duke, T.Y. Cath, L.D. Nghiem, Scaling control during membrane distillation of coal seam gas reverse osmosis brine, J. Membr. Sci., 493 (2015) 673–682.
[18] A. Antony, J.H. Low, S. Gray, A.E. Childress, P. Le-Clech, G. Leslie, Scale formation and control in high pressure membrane water treatment systems: a review, J. Membr. Sci., 383 (2011) 1–16.
[19] P. Zhang, P. Knötig, S. Gray, M. Duke, Scale reduction and cleaning techniques during direct contact membrane distillation of seawater reverse osmosis brine, Desalination, 374 (2015) 20–30.
[20] S. Salvador Cob, C. Yeme, B. Hofs, E.R. Cornelissen, D. Vries, F.E. Genceli Güner, G.J. Witkamp, Towards zero liquid discharge in the presence of silica: stable 98% recovery in nanofiltration and reverse osmosis, Sep. Purif. Technol., 140 (2015) 23–31.
[21] D.M. Warsinger, J. Swaminathan, E. Guillen-Burrieza, H.A. Arafat, J.H. Lienhard V, Scaling and fouling in membrane distillation for desalination applications: a review, Desalination, 356 (2015) 294–313.
[22] S.A. Ali, I.W. Kazi, F. Rahman, Synthesis and evaluation of phosphate-free antiscalants to control $CaSO_4 \bullet 2H_2O$ scale formation in reverse osmosis desalination plants, Desalination, 357 (2015) 36–44.

[23] S. Jamaly, N.N. Darwish, I. Ahmed, S.W. Hasan, A short review on reverse osmosis pretreatment technologies, Desalination, 354 (2014) 30–38.
[24] K. Chauhan, R. Kumar, M. Kumar, P. Sharma, G.S. Chauhan, Modified pectin-based polymers as green antiscalants for calcium sulfate scale inhibition, Desalination, 305 (2012) 31–37.
[25] C. Wildebrand, H. Glade, S. Will, M. Essig, J. Rieger, K.-H. Büchner, G. Brodt, Effects of process parameters and antiscalants on scale formation in horizontal tube falling film evaporators, Desalination, 204 (2007) 448–463.
[26] E. Drioli, G. Di Profio, E. Curcio, Progress in membrane crystallization, Curr. Opin. Chem. Eng., 1 (2012) 178–182.
[27] W. Li, B. Van der Bruggen, P. Luis, Integration of reverse osmosis and membrane crystallization for sodium sulphate recovery, Chem. Eng. Process., 85 (2014) 57–68.
[28] F. Edwie, T.S. Chung, Development of hollow fiber membranes for water and salt recovery from highly concentrated bring via direct contact membrane distillation and crystallization, J. Membr. Sci., 421–422 (2012) 111–123.
[29] S. Lee, J. Kim, C.-H. Lee, Analysis of $CaSO_4$ scale formation mechanism in various nanofiltration modules, J. Membr. Sci., 163 (1999) 63–74.
[30] S. Lee, R.M. Lueptow, Control of scale formation in reverse osmosis by membrane rotation, Desalination, 155 (2003) 131–139.
[31] H.-J. Oh, Y.-K. Choung, S. Lee, J.-S. Choi, T.-M. Hwang, J.H. Kim, Scale formation in reverse osmosis desalination: model development, Desalination, 238 (2009) 333–346.
[32] J. Koo, J. Han, J. Sohn, S. Lee, T.-M. Hwang, Experimental comparison of direct contact membrane distillation (DCMD) with vacuum membrane distillation (VMD), Desal. Water Treat., 51 (2013) 6299–6309.
[33] S. Lee C.-H. Lee, Effect of operating conditions on $CaSO_4$ scale formation mechanism in nanofiltration for water softening, Water Res., 34 (2000) 3854–3866.